

The American Journal of Human Genetics, Volume 104

Supplemental Data

Gene Augmentation and Readthrough

Rescue Channelopathy in an iPSC-RPE Model

of Congenital Blindness

Pawan K. Shahi, Dalton Hermans, Divya Sinha, Simran Brar, Hannah Moulton, Sabrina Stulo, Katarzyna D. Borys, Elizabeth Capowski, De-Ann M. Pillers, David M. Gamm, and Bikash R. Pattnaik

Gene augmentation and read-through rescue channelopathy in an iPSC-RPE model of congenital blindness

Authors: Pawan K. Shahi^{1,2}, Dalton Hermans¹, Divya Sinha^{2,3}, Simran Brar¹, Hannah Moulton¹,
Sabrina Stulo¹, Katarzyna D. Borys³, Elizabeth Capowski^{2,3}, De-Ann M. Pillers^{1,2,4}, David M.
Gamm^{2,3,5}, Bikash. R. Pattnaik^{1,2,5}†

Affiliations:

¹Division of Neonatology, Department of Pediatrics, University of Wisconsin-Madison, Madison
53706

²McPherson Eye Research, University of Wisconsin-Madison, Madison 53705

³Waisman Center, University of Wisconsin-Madison, Madison 53705

⁴Medical Genetics, University of Wisconsin-Madison, Madison 53706

⁵Department of Ophthalmology and Visual Sciences, University of Wisconsin-Madison 53705.

†To whom correspondence should be addressed:

Bikash R. Pattnaik, Ph.D.

Department of Pediatrics, University of Wisconsin

1300 University Avenue, Room 112 SMI, Madison, WI 53706, USA

Tel.: +1 608 265 9486, Fax: +1 608 262 6298

Email: bikashp@pediatrics.wisc.edu

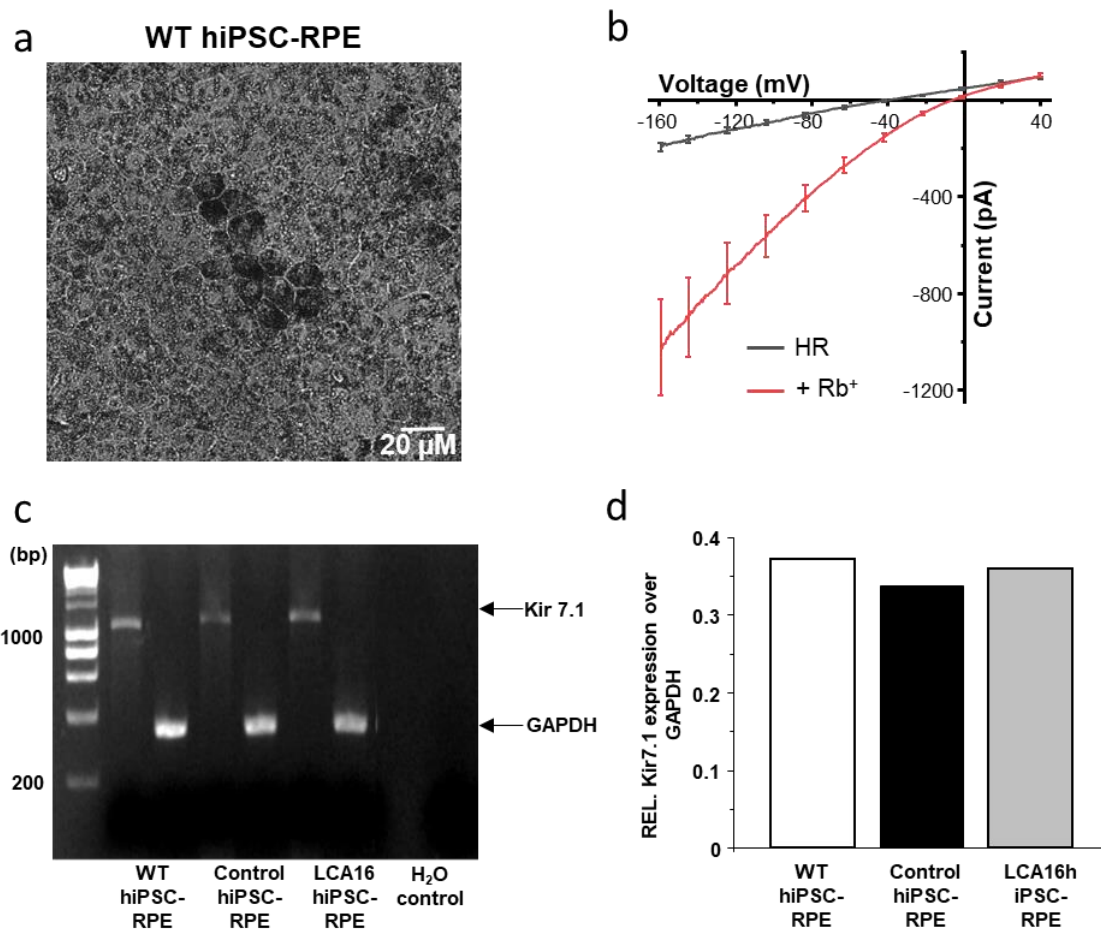


Figure S1

Kir7.1 phenotype in wild-type hiPSC-RPE cells.

(a) Bright field image of wild-type hiPSC-RPE tight monolayer in transwell culture. (b) Whole cell recording in isolated cells to demonstrate Rb⁺ induced increase in Kir7.1 current. (c) Comparison of *KCNJ13* transcripts in wild-type, control and LCA16 hiPSC-RPE cells. For house-keeping gene GAPDH was amplified using forward primer - GTCAGTGGTGGACCTGACCT and reverse primer - TTCCTCTTGTGCTCTTGCTG resulting in a 329 bp product. (d) Comparable *KCNJ13* (relative to GAPDH) transcript expression in wild-type, control, and LCA16 hiPSC-RPE cells.

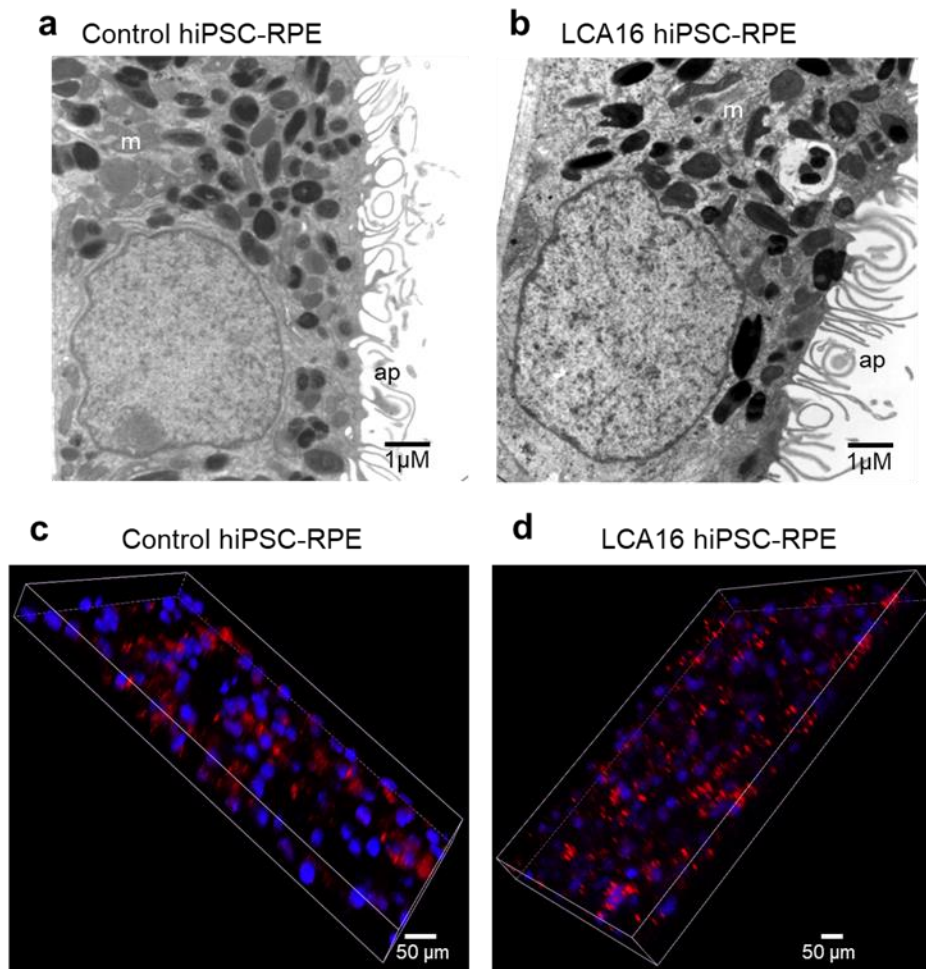


Figure S2

Phenotype of affected individual derived iPSC-RPE cells.

Comparison of electron micrograph of a control hiPSC-RPE cell (a) and an LCA16 hiPSC-RPE cell (b) showing normal columnar morphology with basal infoldings, large nuclei, mitochondria (m), melanosomes and intact apical membrane with extending processes (ap). Images of live control hiPSC-RPE (c) and affected individual derived hiPSC-RPE (d) cells in x-y-z dimension showing POS (red) and nuclei (blue) imaged 6 days after feeding cells for 1 day with fluorescent-labeled bovine POS. More undigested red fluorescent POS particles are visible in LCA16 hiPSC-RPE cells.

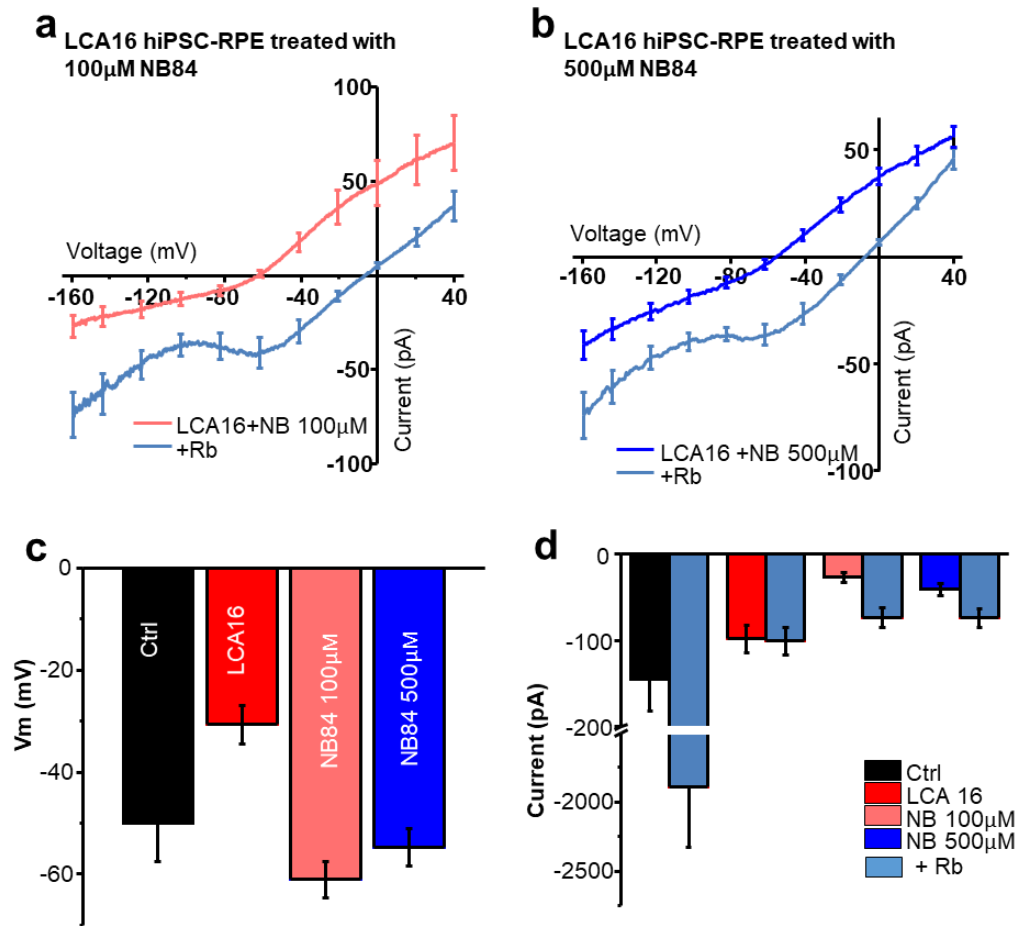


Figure S3

Subpopulation of hiPSC-RPE show rescue in membrane potential but not current amplitude.

a) I/V plot of average current response in a subgroup of LCA16 hiPSC-RPE cells in normal K^+ Ringer's and high Rb^+ Ringer's solution after treatment of cells with 100 μM NB84. b) I/V plot showing K^+ and Rb^+ current response in LCA16 hiPSC-RPE after treatment with 500 μM NB84. c) Average plot of membrane potential showing rescue of membrane potential to control levels after treatment of LCA16 hiPSC-RPE with 100 or 500 μM NB84. d) Current amplitude plot clearly demonstrating no rescue in current amplitude after treatment with either 100 or 500 μM NB84.

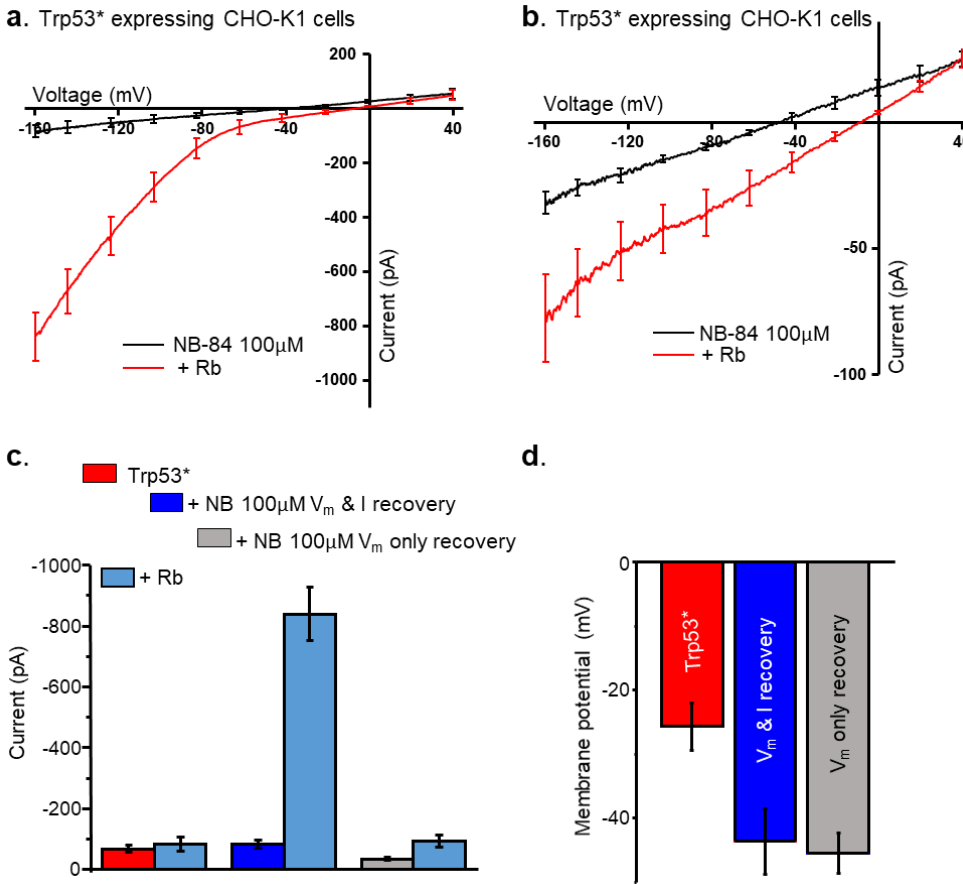


Figure S4

Read-through of Trp53* ectopically expressed in CHO cells. As in LCA16 hiPSC-RPE cells, transduced CHO cells showed inwardly rectifying Kir7.1 current activated by Rb+ only after treatment with NB84. a) I/V plot of cells showing K+ (black) and Rb+ (red) current after treatment with NB84 showing recovery of both current amplitude and membrane potential. b) A group of NB84 treated cells showing somewhat linear I/V plot for K+ (black) and Rb+ (red) illustrating recovery of only membrane potential but not current amplitude. Comparison of average recovery of both current amplitude (c) and membrane potential (d) after treatment of Trp53* expressing CHO cells.

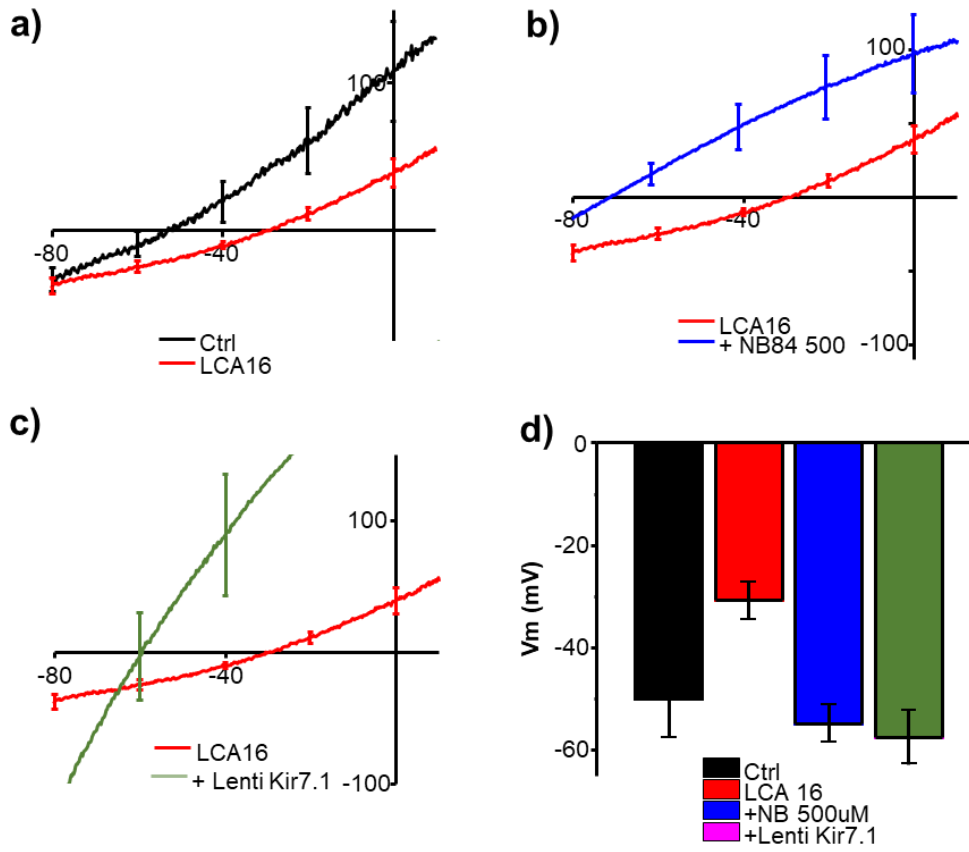


Figure S5

Comparison of the Rescue of membrane potential across treatment modalities. a) On an expanded scale of the x-axis, resting membrane potential of control (black) and LCA16 iPSC-RPE (red) showed a positive shift in I/V plot. b) For the LCA16 iPSC-RPE cells (red trace), treatment with NB84 shifted the I/V-plot to negative (blue). c) Plot of average I/V also showed a negative shift of resting potential after gene augmentation (green). d) Bar graph comparison of resting membrane potential showed recovery of LCA16 iPSC-RPE to control level after treatment with NB84 or upon gene augmentation.

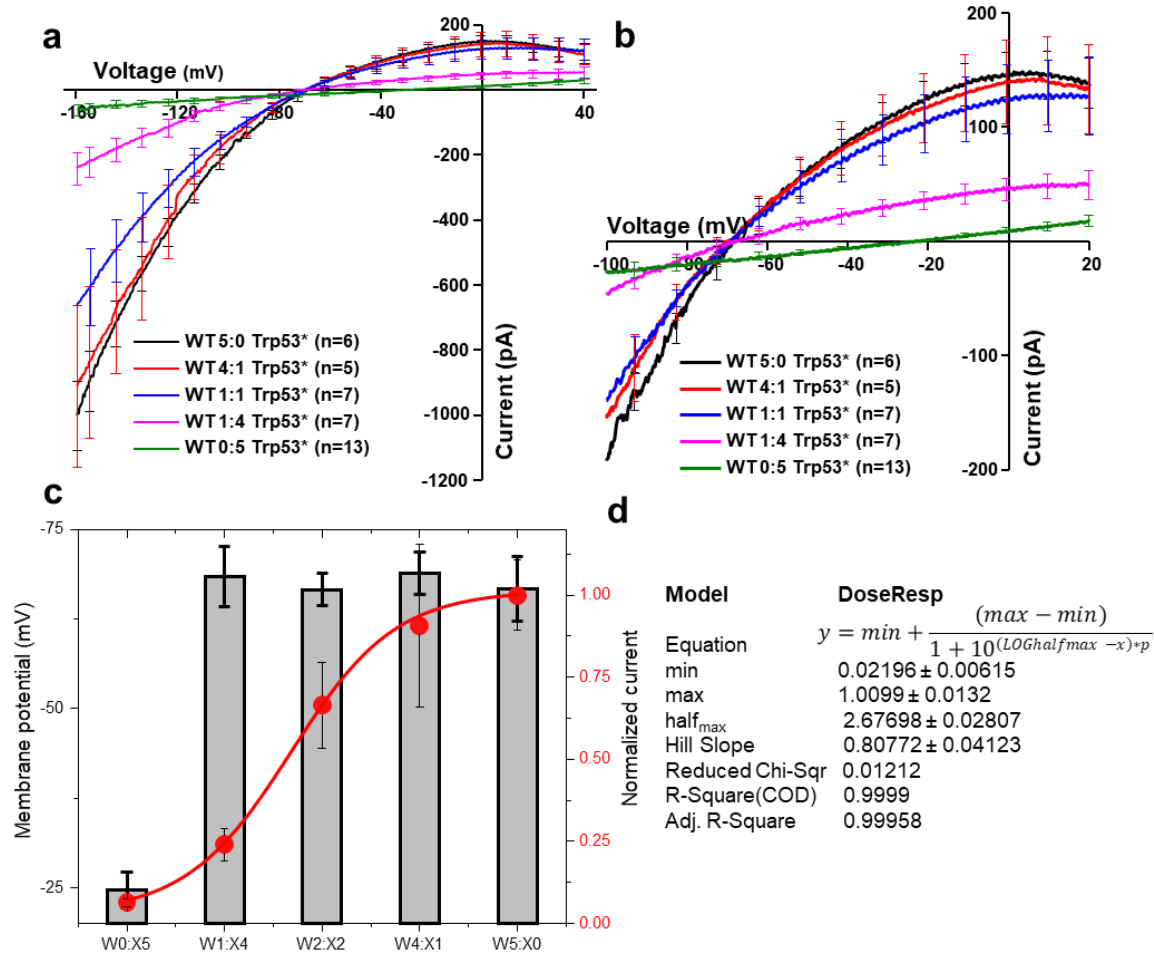


Figure S6

Determination of the extent of wildtype protein expression required for functional rescue.

We were particularly interested in quantitating how much gene augmentation/correction is required to restore channel function. We expressed either Trp53* or wild type Kir7.1 protein alone or in various combinations in CHO cells. a) Current recordings are shown as I/V plots. b) On an expanded scale for x-axis, resting membrane potential shows negative shift with wild type protein making up only 20% of the protein expression. c) Average plot of either normalized current amplitude (filled circles) or membrane potential (grey bar) as a function of increasing wildtype protein expression. Solid line is a best fit for distribution using equation shown on the right. Half-maximum current was obtained with about 26% of the wild type protein expression.

Video

Normal Kir7.1 (green) expression in apical side of the LCA16 hiPSC-RPE cells. Video reconstruction from Z-stack images of LCA16 hiPSC-RPE a week after transduction with lentivirus carrying eGFP-Kir7.1 driven by EF1a promoter. Highlighted are apical and basal sides of the tissue, optical sections, tight junction marked with antiZO-1 antibody (red) and nucleus with DAPI (blue).